PHYSICAL REVIEW B **72**, 241402(R) (2005)

Exciton binding energies in carbon nanotubes from two-photon photoluminescence

J. Maultzsch,[1,*] R. Pomraenke,[2] S. Reich,[3] E. Chang,[4] D. Prezzi,[4] A. Ruini,[4] E. Molinari,[4] M. S. Strano,[5] C. Thomsen,[1] and C. Lienau[2]

[1]*Institut für Festkörperphysik, Technische Universität Berlin, Hardenbergstr. 36, 10623 Berlin, Germany*

[2]*Max-Born-Institut für Nichtlineare Optik und Kurzzeitspektroskopie, 12489 Berlin, Germany*

[3]*Department of Materials Science and Engineering, Massachusetts Institute of Technology, 77 Massachusetts Avenue, Cambridge, Massachusetts 02139-4307, USA*

[4]*INFM National Research Center S3, and Physics Department, University of Modena and Reggio Emilia, 41100 Modena, Italy*

[5]*Deptartment of Chemistry and Biomolecular Engineering, University of Illinois, Urbana, Illinois 61801, USA*

(Received 5 May 2005; revised manuscript received 28 October 2005; published 14 December 2005; publisher error corrected 9 January 2006)

Excitonic effects in the linear and nonlinear optical properties of single-walled carbon nanotubes are manifested by photoluminescence excitation experiments and *ab initio* calculations. One- and two-photon spectra showed a series of exciton states; their energy splitting is the fingerprint of excitonic interactions in carbon nanotubes. By *ab initio* calculations we determine the energies, wave functions, and symmetries of the excitonic states. Combining experiment and theory we find binding energies of 0.3–0.4 eV for nanotubes with diameters between 6.8 and 9.0 Å.

DOI: 10.1103/PhysRevB.72.241402 PACS number(s): 78.67.Ch, 71.15.Qe, 73.22.−f, 78.20.Bh

Single-walled carbon nanotubes are fascinating nano-objects.[1] Their unique geometric, electronic, and optical properties hold promise for a variety of applications, including nanoscale field-effect transistors, electrically excited single-molecule light sources, and nanosensing.[2–4] Initially, their optical properties received comparatively little attention, as photoluminescence is quenched in nanotube bundles by nonradiative relaxation of excited carriers via metallic tubes. This has changed fundamentally since the discovery of band-gap luminescence from individual nanotubes, enabling direct studies of their optical properties.[5–7]

Nanotube optical spectra have mostly been interpreted in terms of single-particle excitations so far,[6] governed by the van Hove singularities in the density of states of a quasi-one-dimensional system. Recent theoretical studies, in contrast, predict that excitonic effects, i.e., the Coulomb interaction between the excited electron and hole, affect both the transition frequencies and the shape of the optical spectra.[8–13] Because of the strong quantum confinement of the electron and hole in the quasi-one-dimensional nanotube, large exciton binding energies are expected, and predicted values range from a few tens of meV to 1 eV, depending on tube diameter, chirality, and dielectric screening.[8–10] The strength of the Coulomb correlation, however, directly influences the optical properties. Also, the existence of optically inactive ("dark") excitonic states may cause the unusually low luminescence quantum yield in nanotubes.[11] Finally, the transport properties of nanotube devices are affected as optical excitations may move either as uncorrelated electrons and holes or as bound excitons.[14]

So far, experimental evidence for excitonic correlations in nanotubes is indirect. Optical absorption and emission energies differ from the single-particle predictions ("ratio problem").[6] Also, ultrafast intersubband relaxation is thought to support the exciton picture.[15,16] In this Communication, we directly identify exciton binding effects in single-walled carbon nanotubes by one- and two-photon luminescence. We calculate the energies and wave functions of one- and two-photon active exciton states from first principles, in excellent agreement with our experiments. Supported by our *ab initio* calculations, we provide a model to estimate exciton binding energies, which are 300–400 meV for the tubes observed in our experiment.

A classical example for two-particle Coulomb correlations is the Rydberg series in atomic hydrogen. The same series governs the bound excitonic states $E^n = E_{\mathrm{gap}} - E^{\mathrm{R}}/n^2$ in homogeneous three-dimensional (3D) semiconductors (E_{gap}: band-gap energy, E^{R}: 3D exciton Rydberg energy). In carbon nanotubes, the electron density is confined to the plane of the rolled graphite sheet. Excitonic wave functions are expected to be delocalized along the circumference and to extend over several nm along the tube axis.[8]

The concept of our experiment is to validate the excitonic character of optical excitations in carbon nanotubes by addressing excitonic states with different symmetry. In the 3D hydrogen model, this would correspond to addressing *s*- and *p*-like states. In carbon nanotubes, one expects for each allowed interband transition a series of transitions to optically active exciton states with odd (u) symmetry with respect to rotations by π about the U axis of the tube [Fig. 1(a)]. Two-photon spectroscopy, on the other hand, couples to the otherwise optically inactive even (g) states [Fig. 1(b)]. The energetic splitting between the one- and two-photon observed states indicates the strength of Coulomb correlations. Therefore, two-photon absorption is an elegant technique to determine excitonic effects.[17]

We investigated single-walled carbon nanotubes suspended in D_2O wrapped by a surfactant.[5] The sample was excited at room temperature with 150 fs pulses from an optical parametric oscillator tunable between 1150 and 2000 nm with an average power of 60 mW. The luminescence was recorded in a 90° configuration by a charge-coupled device (CCD). Between 850 and 1070 nm [Fig.

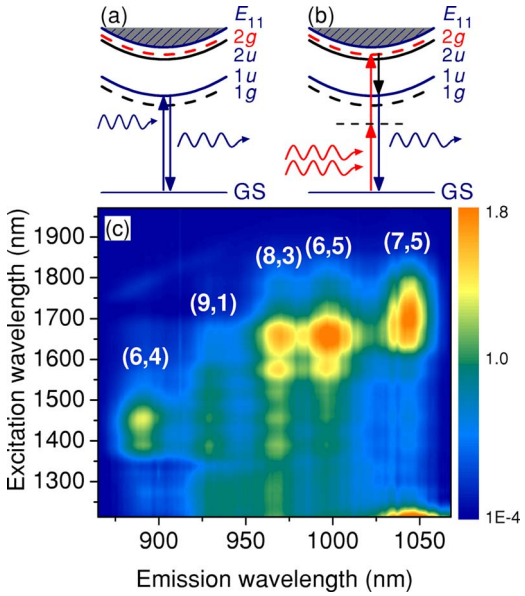

FIG. 1. (Color online) (a) Schematic picture of one-photon absorption and emission in carbon nanotubes. E_{11} indicates the single-particle transition between the lowest subbands. One-photon excitations couple to excitonic states with odd (u) symmetry with respect to π rotations about the U axis. The U axis is perpendicular to the tube axis through the center of the C hexagons (Ref. 18). (1) and (2) indicate the symmetry of the envelope function with respect to reflection in the $z=0$ plane (see Fig. 4). Emission occurs from the lowest one-photon active $1u$ state. (b) Two-photon absorption results in the excitation of exciton states with even (g) symmetry under the U-axis operation. (c) Two-photon luminescence spectra of carbon nanotubes. The luminescence intensity is plotted as a function of excitation and detection wavelength.

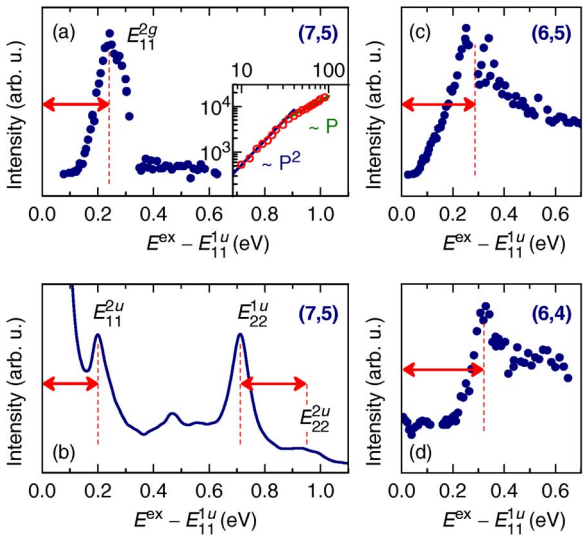

FIG. 2. (Color online) (a) Two-photon luminescence intensity of the (7,5) tube (at 1045±5 nm) as a function of excitation energy E^{ex}. The abscissa gives the difference between two-photon absorption and emission energy. The $2g$ state is excited at 0.24 eV above the $1u$ emission. Inset: Excitation-power (in mW) dependence of luminescence intensity. (b) Same as in (a) but for one-photon absorption. E_{11} and E_{22} indicate the first- and second-subband transitions, respectively. The peak at 0.2 eV is assigned to the $2u$ exciton resonance. (c) and (d) Two-photon luminescence excitation spectra of the (6,5) and the (6,4) tubes, respectively.

1(c)], we identified the luminescence from five different nanotube species [(6,4), (9,1), (8,3), (6,5), and (7,5)]. We also observed the weak emission from the (9,4) tube at 1130 nm. (Ref. 19) The assignment of chiral indices (n_1,n_2) is based on Raman[20] and luminescence[6] data.

Figure 1(c) shows the luminescence for excitation below the band gap between 1210 and 1970 nm. For each tube we find a maximum in the luminescence intensity at an excitation wavelength far above the emission wavelength, but significantly smaller than twice this wavelength. We assign these absorption maxima to resonant two-photon excitation of the lowest two-photon allowed exciton state ($2g$). The positions of the maxima thus correspond to half the energy of this state. Emission results from relaxation into the lowest one-photon active $1u$ state [Fig. 1(b)]. The shift of about 240–320 meV between both states is a signature of (i) the excitonic nature of absorption and emission at room temperature, and (ii) exciton binding energies of almost one-fourth of the band-gap energy. An analyis of the power dependence of the emission intensity supports the assignment to two-photon absorption [inset of Fig. 2(a)]. At low excitation powers, the luminescence increases quadratically and saturates into a linear increase above 40 mW.

To quantitatively analyze the splitting between the one- and two-photon allowed transitions, we plot two-photon luminescence excitation spectra for different nanotubes [Figs. 2(a), 2(c), and 2(d)]. They show the emission intensity as a function of the energy difference $E^{ex}-E_{11}^{1u}$ between two-photon excitation and emission energy. For the (7,5) tube [Fig. 2(a)], the resonance maximum is at 240 meV above the one-photon active state. For the (6,5) and (6,4) tubes [Figs. 2(c) and 2(d)], the $E_{11}^{2g}-E_{11}^{1u}$ splittings are 285 and 325 meV, respectively. Similar experimental results have been recently reported for the (7,5), (6,5), and (8,3) tube.[21]

We expect to observe a second weakly one-photon allowed absorption resonance close to the two-photon active state. In Fig. 2(b), we plot a one-photon luminescence excitation spectrum of the (7,5) tube. The spectrum shows an absorption resonance at an excess energy of 200 meV, i.e., slightly below the first two-photon resonance at 240 meV. The same resonance is also observed in the excitation spectrum of the second subband (E_{22}). These resonances reflect one-photon excitation of higher-lying exciton states. This supports a previous assignment of one-photon excitation spectra,[22] whereas alternative suggestions for the origin of these peaks, including phonon sidebands and exciton-phonon excitations,[23,24] seem less likely.

To confirm the interpretation of our experimental results, we perform a first-principles calculation of excited states for isolated nanotubes. We start from single-particle wave functions obtained by density-functional theory and adopt the *GW* approximation for the self-energy operator.[25] The optical properties are calculated by solving the Bethe–Salpeter equation (BSE) expanded in a localized Gaussian basis set which is symmetric with respect to the screw axis of the tube. This approach permits the calculation of the wave functions and binding energies of bound electron-hole pairs,[26–29] and gives

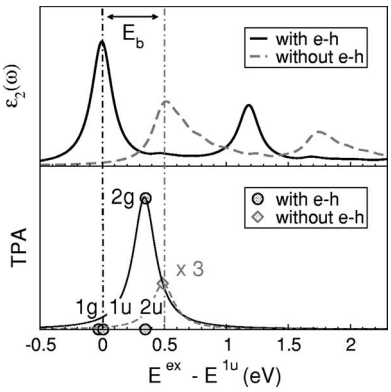

FIG. 3. *Ab initio* calculated (top) one-photon and (TPA, bottom) two-photon absorption for the (6,4) tube with a Lorentzian broadening of 0.1 eV. Black (gray) lines are with (without) electron-hole (e-h) interactions. Bottom: probability amplitude of two-photon scattering to the exciton states $1g$, $1u$, $2u$, and $2g$ (black circles); probability amplitude of scattering to the final state without e-h interaction (gray diamond). Higher-energy states with negligible amplitude are omitted for clarity.

a symmetry characterization of excited states including optical selection rules.

We compute the two-photon absorption intensity versus the energy of the final excited state in the (6,4) tube in Fig. 3. The two inequivalent C atoms of each hexagon lead to a doubling of states with respect to a simple hydrogenlike model, with the states in each doublet being close in energy. We find four bound exciton states below the single-particle gap (gray line), with binding energies of 0.54 ($1g$), 0.50 ($1u$), 0.16 ($2g$), and 0.16 eV ($2u$). (Ref. 30) Their parities under rotation about the U axis are consistent with the fact that the u states are one-photon active and the g states are two-photon allowed. The envelope functions of the strongly bound states ($1g$,$1u$) are approximately symmetric (1) under reflection in the $z=0$ plane; the weakly bound states ($2g$,$2u$) have an approximately antisymmetric (2) envelope and a nodal plane in $z=0$. The most strongly bound exciton state is optically inactive in one-photon absorption because of the even (g) total wave function and weak in two-photon absorption because of the just approximately even (1) envelope.[11] This may explain the small luminescence quantum yield in carbon nanotubes observed at low temperatures.

If we neglect the electron-hole interaction, the two-photon absorption is very close in energy to the first one-photon active state (gray dashed curves in Fig. 3). In contrast, if the electron-hole interaction is included, the energies E_{11}^{2g} and E_{11}^{1u} differ by 0.34 eV, which agrees well with the measured value of 0.325 eV (Table I). The *ab initio* calculation gives a binding energy of 0.5 eV for the (6,4) tube. The lowest exciton wave function extends over several nm along the tube axis and is delocalized along the circumference. The higher exciton states ($2g$,$2u$) are more extended along the tube axis and have a nodal plane at $z=0$ (see Fig. 4). The calculated wave functions are thus Wannier-like and weakly dependent on the circumference direction. Furthermore, the calculated band structure confirms that a two-band model is appropriate.[8]

TABLE I. Observed nanotube structures with their diameter d, emission energy (E_{11}^{1u}), and two-photon absorption energy (E_{11}^{2g}). The binding energy is estimated within the cylinder model (Ref. 31). The fitted values for ϵ are (top to bottom) 10.5, 10.1, 10.6, 11.0, 12.2, and 9.7.

(n_1,n_2)	d (Å)	E_{11}^{1u} (eV) Expt.	E_{11}^{2g} (eV) Expt.	$E_{11}^{2g}-E_{11}^{1u}$ (eV) Expt.	E_{11}^{b} Theor.
(6,4)	6.83	1.395	1.720	0.325	0.42
(9,1)	7.47	1.335	1.650	0.315	0.42
(8,3)	7.72	1.275	1.570	0.295	0.38
(6,5)	7.47	1.245	1.530	0.285	0.37
(7,5)	8.18	1.190	1.430	0.240	0.31
(9,4)	9.03	1.095	1.375	0.280	0.38

Based on our *ab initio* analysis, we introduce a variational model to estimate exciton binding energies from the splitting $E_{11}^{2g}-E_{11}^{1u}$. It describes an electron and hole moving under attractive Coulomb interaction on a cylinder surface,[31] with a Coulomb potential given by $V(z,\theta,R)=e^2/\epsilon\sqrt{z^2+R^2\cos^2(\theta/2)}$ with the relative coordinate (z,θ) and tube diameter $2R$. Even- and odd-parity trial wave functions, $\psi_1(z;a)=\exp(-a|z|)$ and $\psi_2(z;a)=z\exp(-a|z|)$ respectively, are chosen on the basis of the *ab initio* excitonic wave functions. The dielectric constant ϵ is adjusted such that $E_{11}^{2g}-E_{11}^{1u}$ matches the experimental value. For example, for the (6,4) tube we obtain a binding energy $E^b=0.42$ eV with $\epsilon\approx 10.5$ (Table I).

From the variational model and previous theoretical work,[10–12] we expect an increase of the exciton binding energy with decreasing tube diameter. The energy should also depend on the family index (Ref. 32) $\nu=(n_1-n_2)\bmod 3=\pm 1$, with larger binding energies E_{11}^{b} for $\nu=-1$ tubes than for $\nu=+1$ tubes with a similar diameter.[10,11] Our experimental results show an overall decrease for larger tube diameters (Table I). All tubes in our experiment have $\nu=-1$, except for the (6,5) tube. It has the same diameter as the (9,1) tube, but a lower binding energy. Our data support the predicted trends;[8–12] a final conclusion may be drawn once a larger

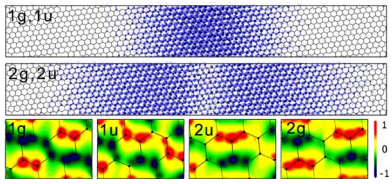

FIG. 4. (Color online) Lowest-energy excitonic wave functions for the (6,4) tube from *ab initio* calculations. The top two panels correspond to the $1g$, $1u$ and $2g$, $2u$ states, respectively, and show the probability of finding the electron on the tube surface when the hole is fixed at the center of the panel ($z=0$). The vertical direction corresponds to the circumference (2.1 nm) and the horizontal direction to the tube axis (15.9 nm). The bottom four panels are blowups of the same states. They display the wave-function amplitude of the electron when the hole is placed in the center of the bond at $z=0$ and show the parity under rotation by π about the U axis. The color (gray) scale is in arbitrary units.

number of species has been studied.

In conclusion, we observed a series of exciton states with different wave-function symmetry in carbon nanotubes by one- and two-photon luminescence. By *ab initio* calculations of one- and two-photon spectra we showed that the experiments can only be interpreted in terms of excitonic effects. Based on these results we introduced a simplified cylindrical model for the excitonic states to derive exciton binding energies from two-photon experiments. We determined binding energies between 300 and 400 meV for several nanotube species. Our results demonstrate that excitonic properties dominate optical absorption and emission in carbon nanotubes even at room temperature.

This work was supported in part by the DFG (Grant No. SFB296), by an INFM Supercomputing grant at Cineca (Italy), by the RTN EU Contract "EXCITING" No. HPRN-CT-2002-00317, and by the Engineering and Physical Sciences Research Council (EPSRC). S.R. was supported by the Oppenheimer Fund and Newnham College. We thank A. Calzolari and G. Bussi for helpful discussions.

*Electronic address: janina@physik.tu-berlin.de

[1] S. Reich, C. Thomsen, and J. Maultzsch, *Carbon Nanotubes: Basic Concepts and Physical Properties* (Wiley-VCH, Berlin, 2004).

[2] S. J. Tans, A. Verschueren, and C. Dekker, Nature (London) **393**, 6680 (1998).

[3] J. A. Misewich, R. Martel, J. C. Tsang, S. Heinze, and J. Tersoff, Science **300**, 783 (2003).

[4] E. S. Snow, F. K. Perkins, E. J. Houser, S. C. Badescu, and T. L. Reinecke, Science **307**, 1942 (2005).

[5] M. J. O'Connell *et al.*, Science **297**, 593 (2002).

[6] S. M. Bachilo, M. S. Strano, C. Kittrell, R. H. Hauge, R. E. Smalley, and R. B. Weisman, Science **298**, 2361 (2002).

[7] A. Hartschuh, H. N. Pedrosa, L. Novotny, and T. D. Krauss, Science **301**, 1354 (2003).

[8] E. Chang, G. Bussi, A. Ruini, and E. Molinari, Phys. Rev. Lett. **92**, 196401 (2004).

[9] C. D. Spataru, S. Ismail-Beigi, L. X. Benedict, and S. G. Louie, Phys. Rev. Lett. **92**, 077402 (2004).

[10] V. Perebeinos, J. Tersoff, and P. Avouris, Phys. Rev. Lett. **92**, 257402 (2004).

[11] H. Zhao and S. Mazumdar, Phys. Rev. Lett. **93**, 157402 (2004).

[12] C. L. Kane and E. J. Mele, Phys. Rev. Lett. **93**, 197402 (2004).

[13] T. Ando, J. Phys. Soc. Jpn. **66**, 1066 (1997).

[14] M. Freitag, J. Chen, J. Tersoff, J. C. Tsang, Q. Fu, J. Liu, and P. Avouris, Phys. Rev. Lett. **93**, 076803 (2004).

[15] O. J. Korovyanko, C.-X. Sheng, Z. V. Vardeny, A. B. Dalton, and R. H. Baughman, Phys. Rev. Lett. **92**, 017403 (2004).

[16] Y.-Z. Ma, L. Valkunas, S. L. Dexheimer, S. M. Bachilo, and G. R. Fleming, Phys. Rev. Lett. **94**, 157402 (2005).

[17] R. Rinaldi, R. Cingolani, M. Lepore, M. Ferrara, I. M. Catalano, F. Rossi, L. Rota, E. Molinari, P. Lugli, U. Marti, D. Martin, F. Morier-Gemoud, P. Ruterana, and F. K. Reinhart, Phys. Rev. Lett. **73**, 2899 (1994).

[18] M. Damnjanović, I. Miloević, T. Vuković, and R. Sredanović, Phys. Rev. B **60**, 2728 (1999).

[19] The emission energies are about 25 meV smaller than reported by Bachilo *et al.* (Ref. 6), which is probably due to the presence of small bundles in our sample.

[20] H. Telg, J. Maultzsch, S. Reich, F. Hennrich, and C. Thomsen, Phys. Rev. Lett. **93**, 177401 (2004).

[21] F. Wang, G. Dukovic, L. E. Brus, and T. Heinz, Science **308**, 838 (2005).

[22] S. Reich *et al.* (unpublished).

[23] V. Perebeinos, J. Tersoff, and P. Avouris, Phys. Rev. Lett. **94**, 027402 (2005).

[24] X. Qiu, M. Freitag, V. Perebeinos, and P. Avouris, Nano Lett. **5**, 479 (2005).

[25] L. Hedin, Phys. Rev. **139**, A796 (1965).

[26] The standard plane-wave formulation of BSE for nanotubes scales like $\sim TR^4 \log(TR^2)$ (R: tube radius; T: length of the unit cell). It is inapplicable to tubes with large unit cells like the (6,4). The typical scaling of our symmetry based formulation is faster ($\sim R^2$) and independent of T.

[27] A. Ruini, M. J. Caldas, G. Bussi, and E. Molinari, Phys. Rev. Lett. **88**, 206403 (2002).

[28] L. X. Benedict, E. L. Shirley, and R. B. Bohn, Phys. Rev. Lett. **80**, 4514 (1998).

[29] S. Albrecht, L. Reining, R. Del Sole, and G. Onida, Phys. Rev. Lett. **80**, 4510 (1998).

[30] Binding energies are defined with respect to the onset of the single-particle continuum (gray line in Fig. 3).

[31] See EPAPS Document No. E-PRBMDO-72-R12548 for a description of the cylinder model. This document can be reached via a direct link in the online article's HTML reference section or via the EPAPS homepage (http://www.aip.org/pubservs/epaps.html).

[32] S. Reich and C. Thomsen, Phys. Rev. B **62**, 4273 (2000).